Extended Abstracts of the 2008 International Conference on Solid State Devices and Materials, Tsukuba, 2008, pp. 896-897

C-7-1

Low-Loss Magnetic Films of Ni-Zn Ferrite by Low-Temperature PVD Method for RF-CMOS Application

Kishou Kaneko, Naoya Inoue, Naoya Furutake, Ken-ichiro Hijioka, Yoshihiro Hayashi

LSI Fundamental Research. Laboratory, NEC Electronics Corporation
1120 Shimokuzawa, Sagamihara, Kanagawa 229-1198, Japan
Phone: +81-42-771-0689 Fax: +81-42-771-0692 e-mail: kishou.kaneko@necel.com

1. Introduction

Integration of magnetic materials is expected to improve the performance of on-chip inductors [1,2] as well as to suppress EMI noises [3] in RF-CMOS LSIs (Fig. 1). Here, not only high magnetic permeability (μ) but also high resistivity (ρ) is needed to reduce eddy-current loss in the magnetic film. Although it is known that NiZn spinel ferrite ($Ni_{1-x}Zn_xFe_2O_4$) has high resistivity, the formation temperature by solid-state reaction is too high to be integrated in LSI interconnects.

In this paper, the NiZn ferrite film is deposited by low temperature RF sputtering method, and the magnetic and electrical properties are investigated with relation to the film microstructure. The effect of the high-ρ ferrite film on on-chip inductor is confirmed by an electro-magnetic field simulation (HFSS).

2. Experimental

NiZn ferrite thin films were deposited by RF magnetron sputtering with Ar/O_2 mixture on 8-inch Si wafers (Fig. 2). The target was a sintered $Ni_{0.5}Zn_{0.5}Fe_2O_4$ ferrite with spinel structure. Since the ferrite film properties were independent of substrate temperature ranged from 300 to 500 ^oC, we selected 300 ^oC in the following experiments. This low temperature process is applicable for the Cu/Low-k BEOL process. In this work, we investigated the relation between the electrical/magnetic properties and the film microstructure, which is controlled by (1) the buffer layers inserted under the ferrite film and (2) the sputtering condition such as O_2/Ar gas ratio (Table.1). Fig. 3 shows schematic illustration of the sample structure, in which three types of buffer layers such as SiO_2, Ti(002) and TaN(110) were investigated. Fig.3 includes also evaluation methods in this work. The microstructure of the film was characterized by SEM and XRD. VSM (Vibrating Sample Magnetometer) with applying in-plane magnetic field measures magnetic property. Thermally evaporated Au electrode was deposited to measure the electric resistivity of the film. Finally, inductor performance was simulated as a function of the electric resistivity of magnetic film, covering the inductor..

3. Effects of Buffer Layer

The XRD analysis revealed that the buffer layer determined the crystal structure of the sputtered spinel film (Fig.4). Peak intensity of spinel (311) was higher on the TaN buffer than on the amorphous SiO_2. Ti-buffer enhanced $(111)_{spinel}$ orientation, instead of $(311)_{spinel}$. The structure of $(311)_{spinel}$ plane probably matches that of $(110)_{TaN}$ plane, enhancing $(311)_{spinel}$ orientation.

Magnetic hysteresis loop also depended on the buffer layer, or essentially the crystal orientation (Fig.5). The ferrite film with strong $(311)_{spinel}$ orientation on the TaN buffer had lower coercivity (H_c) and higher saturation magnetization (M_s) than those on the other buffers. High $(111)_{spinel}$ orientation of the ferrite on the Ti buffer is not related to the magnetic property. Cross-sectional SEM image of the $(311)_{spinel}$-orientated ferrite film with TaN buffer revealed that the ferrite film had a clearly columnar structure aligned perpendicular to the film plane (Fig. 6).

4. Effects of Sputtering Conditions

The XRD peak intensity of $(311)_{spinel}$ depended on the mixture ratio of Ar/O_2 in the sputtering gas, not on the partial pressure of O_2 (Fig. 7). It was found that 8%-O_2 was the optimum condition for the ferrite crystallization. In the low O_2 region, oxygen supply was too low to be crystallized. Excess oxygen also suppresses the ferrite crystallization. Magnetic property correlated with the ferrite $(311)_{spinel}$ peak intensity, and the (311) preferred crystal structure was essential to achieve high magnetization (Fig. 8).

Fig.9 shows the I-V curves for the MIM structure with ferrite as an insulator. The ferrite film sputtered under O_2 addition less than 4% was highly conductive or low-ρ. Introduction of oxygen vacancy, due to low oxygen supply, increases the electric conduction. While, high O_2 content greater than 8% increased resistivity by 10^4 times.

Namely, RF sputtering of NiZn-ferrite with high oxygen supply (>8%) on the TaN buffer improves both magnetic and electric properties, due to well crystallized (311) phase and sufficient oxidation even at low temperature such as 300 ^oC.

5. Integration of high-ρ magnetic film effect

Inductor performance was simulated for the 3D inductor (M2-M5) [4] with a magnetic cover over the inductor (Fig.10). Here, high-ρ (10^7 Ω-cm) film with μ=2 in this work and low-ρ (10 μΩ-cm) film with high μ=100, assumed as Permalloy (Ni-Fe), were compared to check the effect of resistivity. The high-ρ integrated magnetic film enhanced the intensity of magnetic field around the inductor at 10GHz (Fig. 11(a)). The low-ρ integrated magnetic film, on the other hand, degraded the intensity regardless of the high-μ (Fig.11(b)). The inductor with a low-ρ magnetic core had high eddy current loss, resulting in low efficiency at 10GHz.

For the RF applications, high-ρ magnetic core should be integrated to attenuate the eddy currents and extend the inductor usable frequency range.

6. Conclusions

Magnetic and electric properties of NiZn ferrite film by the low-temperature RF sputtering were evaluated, relating with the microstructure. . The TaN buffer film and adequate O_2 addition provide a NiZn ferrite film with highly (311) preferred orientation, increasing the saturation magnetization with keeping the film resistivity high. The integrated high-ρ magnetic film is suitable for high-efficiency inductor especially over GHz ranges.

References

[1] Donald S. Gardner, et al., IEEE IEDM2006,p221(2006)
[2] M. Yamaguchi et al, IEEE Trans Magn.p351(2005)
[3] K.Kondo, et al., J.Appl.Phys., 93 ,7130 (2003)
[4] K.Hijioka, et al., Jpn.J.Appl.Phys.,47 ,p2477(2008).

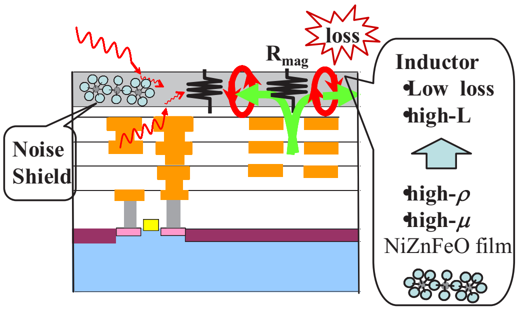

Fig.1 High-μ magnetic material with high resistivity (ρ) is a promising candidate for low loss inductors as well as noise filters. The ferrite process should be compatible with the Cu/low-k BEOL process less than 350°C.

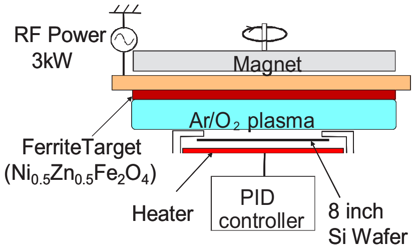

Fig.2 Schematic diagram of RF magnetron sputtering system to sputter the ferrite film. Target was a sintered $Ni_{0.5}Zn_{0.5}Fe_2O_4$ ferrite with spinel structure, and its diameter was 12"ϕ for 8-inches wafer process.

Table.1 Sputtering condition for ferrite films and the buffer layers under the ferrite film.

Substrate Temperature	300℃
RF Power	3kW
O_2/Ar ratio	**0,4,8,12%**
Pressure	3.2mTorr
Buffer layer	**SiO_2,TaN,Ti**
Buffer layer Thickness	100nm
Ferrite Thickness	200nm

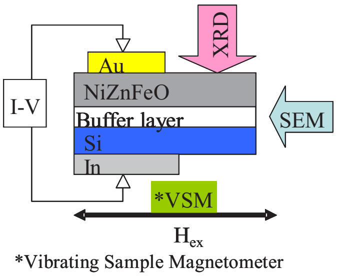

Fig.3 Schematic illustration of the evaluation structure.

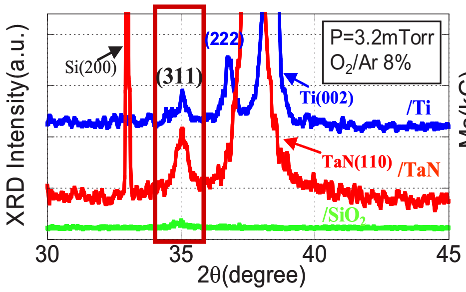

Fig.4 XRD spectra for ferrite on various buffer films such as SiO_2, Ti and TaN. The crystal orientation of the ferrite depended on the buffer layer.

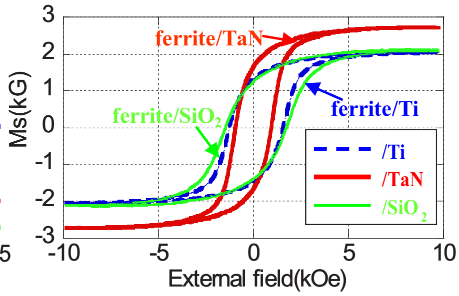

Fig.5 Magnetic hysteresis loops for the ferrite films on the different buffers. The TaN buffer improves the magnetic properties.

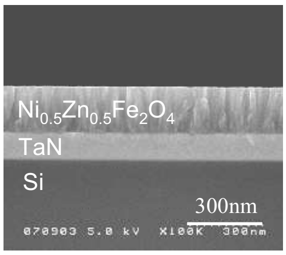

Fig.6 Cross sectional SEM image of sputtered NiZn-ferrite on the TaN film.

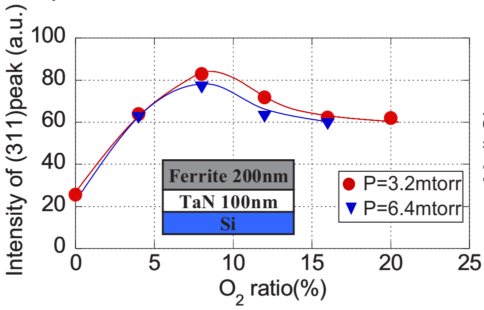

Fig.7 Intensity of (311) peak vs. O_2/Ar ratio in the sputtering gas. The intensity is independent of pressure. The 8%-O_2 was the most suitable condition for (311) crystal orientation of spinel ferrite.

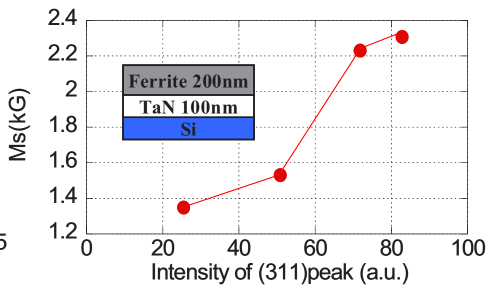

Fig.8 Saturation Magnetization (M_s) vs. intensity of $(311)_{spinel}$ peak. High intensity of (311) spinel phase was an essential to achieve high M_s.

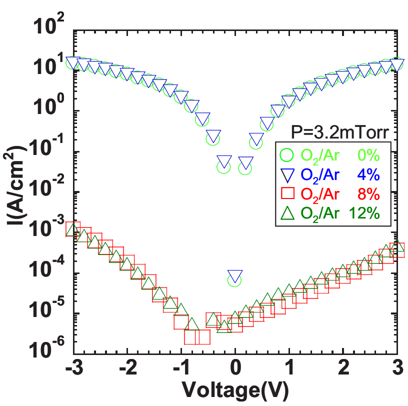

Fig.9 Current density as a function of voltage for the ferrite/TaN film. Ferrite was high-ρ insulator at 8, 12%-O_2 conditions, while it was very low-ρ conductor with 0, 4%-O_2 conditions.

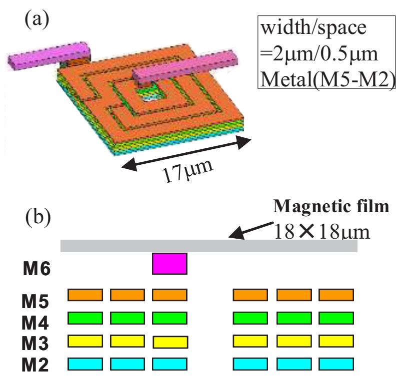

Fig.10 Schematic illustration of 3D inductor for the simulation; (a) birds-eye view, and (b) cross-sectional structure of inductor with magnetic film. 500nm-thick magnetic film is put on M6, covering the inductor area.

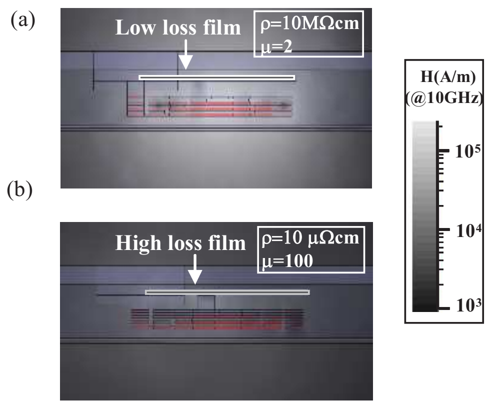

Fig.11 Simulated magnetic field distribution at 10GHz around 3D inductors: (a) with low loss (high-ρ) magnetic film, and (b) with high loss (low-ρ) magnetic film. Low loss magnetic film (high-ρ) successfully enhances the intensity of magnetic field, while high loss film degrades magnetic field by high eddy current loss.